iScience

CellPress

Article

HIF-mediated Suppression of DEPTOR Confers Resistance to mTOR Kinase Inhibition in Renal Cancer

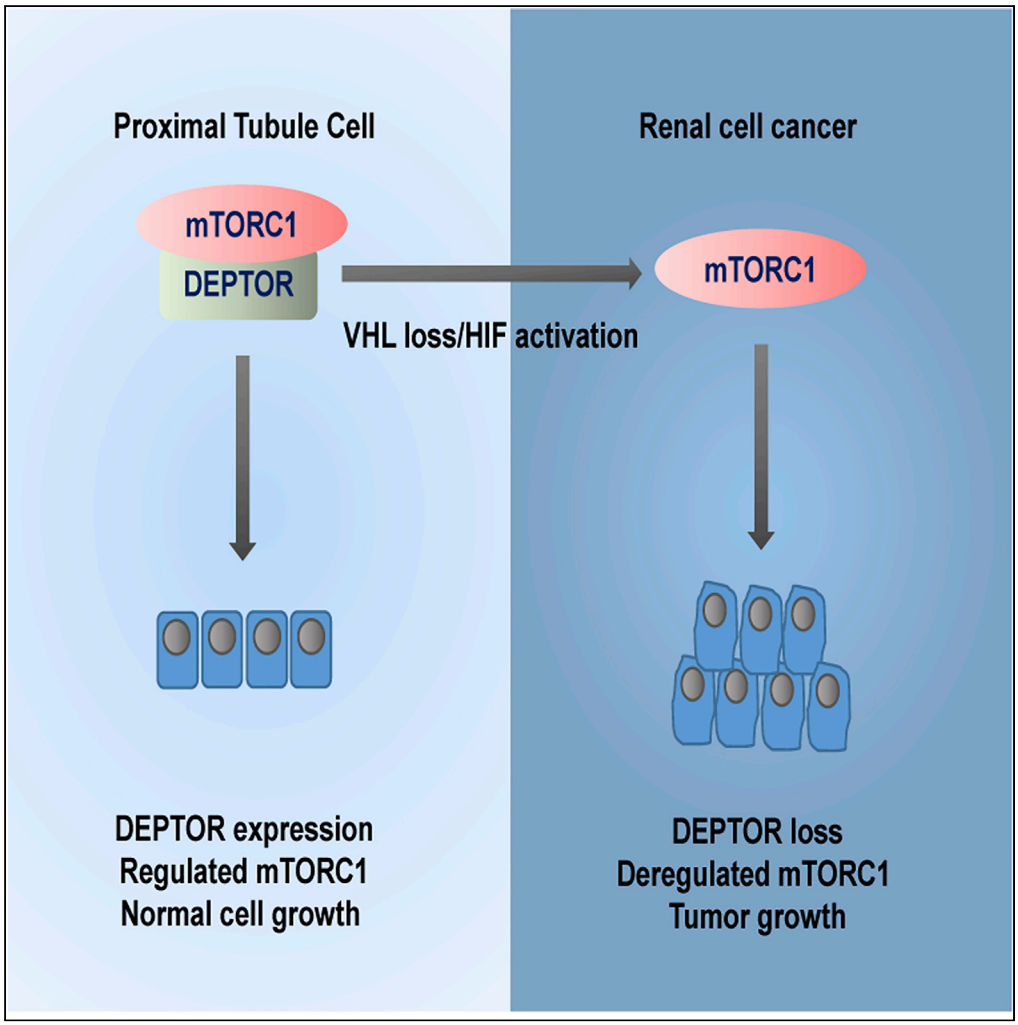

Hong Doan, Alexander Parsons, Shruthi Devkumar, Jogitha Selvarajah, Francesc Miralles, Veronica A. Carroll

vcarroll@sgul.ac.uk

HIGHLIGHTS

DEPTOR is suppressed in VHL-inactivated renal cell carcinoma

HIF-α mediates DEPTOR suppression via BHLHe40

Loss of DEPTOR leads to deregulated mTORC1 negative feedback to IRS-2/PI3K/Akt

DEPTOR loss leads to resistance to mTOR kinase inhibition

Doan et al., iScience *21*, 509–520
November 22, 2019
https://doi.org/10.1016/j.isci.2019.10.047

iScience

CellPress

Article

HIF-mediated Suppression of DEPTOR Confers Resistance to mTOR Kinase Inhibition in Renal Cancer

Hong Doan,[1] Alexander Parsons,[1] Shruthi Devkumar,[1,2] Jogitha Selvarajah,[1,2] Francesc Miralles,[1,2] and Veronica A. Carroll[1,2,3,*]

SUMMARY

Mechanistic target of rapamycin (mTOR) is a fundamental regulator of cell growth, proliferation, and metabolism. mTOR is activated in renal cancer and accelerates tumor progression. Here, we report that the mTOR inhibitor, DEP domain-containing mTOR-interacting protein (DEPTOR), is strikingly suppressed in clear cell renal cell carcinoma (ccRCC) tumors and cell lines. We demonstrate that DEPTOR is repressed by both hypoxia-inducible factors, HIF-1 and HIF-2, which occurs through activation of the HIF-target gene and transcriptional repressor, BHLHe40/DEC1/Stra13. Restoration of DEPTOR- and CRISPR/Cas9-mediated knockout experiments demonstrate that DEPTOR is growth inhibitory in ccRCC. Furthermore, loss of DEPTOR confers resistance to second-generation mTOR kinase inhibitors through deregulated mTORC1 feedback to IRS-2/PI3K/Akt. This work reveals a hitherto unknown mechanism of resistance to mTOR kinase targeted therapy that is mediated by HIF-dependent reprograming of mTOR/DEPTOR networks and suggests that restoration of DEPTOR in ccRCC will confer sensitivity to mTOR kinase therapeutics.

INTRODUCTION

Mechanistic target of rapamycin (mTOR) is a Ser/Thr protein kinase belonging to the phosphoinositide-3-kinase-related kinase (PIKK) family that regulates diverse cellular processes including cell growth, metabolism, and survival in response to nutrient and growth factor cues (Saxton and Sabatini, 2017). mTOR is part of two functionally distinct protein complexes, mTORC1 and mTORC2, which have multiple components but are primarily characterized by addition of the accessory proteins, regulatory-associated protein of mTOR (Raptor), and rapamycin-insensitive companion of mTOR (Rictor) for mTORC1 and mTORC2, respectively (Saxton and Sabatini, 2017). Both complexes contain an inhibitory subunit, DEP domain-containing mTOR-interacting protein (DEPTOR) (Caron et al., 2018; Peterson et al., 2009). The expression of DEPTOR is tightly controlled and dependent on growth factor signals that suppress DEPTOR levels transcriptionally and by posttranslational modification (Peterson et al., 2009). Mitogenic signals lead to rapid DEPTOR phosphorylation on multiple sites, some of which are dependent on mTOR activity, and DEPTOR is subsequently targeted for proteasomal degradation by $SCF^{\beta TrCP}$ E3 ubiquitin ligase (Duan et al., 2011; Gao et al., 2011; Zhao et al., 2011). Therefore, mTOR and DEPTOR work in a reciprocal manner, each negatively regulating the expression of the other, depending on growth factor cues and nutrient status. Further work has demonstrated that DEPTOR is critical in maintaining mTORC1 homeostasis by regulating mTORC1 negative feedback signaling to insulin receptor substrate 1 (IRS-1) (Caron et al., 2017; Laplante et al., 2012; Peterson et al., 2009).

Increased mTOR pathway activity is frequently observed in cancers with either mutations found in *MTOR* (Grabiner et al., 2014) or components of the PI3K/Akt signaling pathway (Zhang et al., 2017). In clear cell renal cell carcinoma (ccRCC), which is the most common type of kidney cancer, mTORC1 pathway is commonly activated *in vivo* (Pantuck et al., 2007). As such, allosteric mTORC1 inhibitors are approved therapeutic agents as second-line therapy following anti-angiogenic therapy. However, second-generation mTOR kinase inhibitors and dual PI3K/Akt/mTOR targeted therapies have failed to work in ccRCC as expected; the reasons for this are unclear (Powles et al., 2016a, 2016b). The majority of ccRCC tumors are characterized by inactivation of the von Hippel-Lindau tumor suppressor protein (pVHL), which is part of an E3 ligase complex (Shen and Kaelin, 2013). Defective pVHL leads to stabilization of hypoxia-inducible factors, HIF-1α and HIF-2α, that regulate transcription of numerous genes involved in cell

[1]Vascular Biology Research Centre, Molecular and Clinical Sciences Research Institute, St George's, University of London, London SW17 0RE, UK

[2]Centre for Biomedical Education, Institute of Medical and Biomedical Education, St George's, University of London, London SW17 0RE, UK

[3]Lead Contact

*Correspondence: vcarroll@sgul.ac.uk

https://doi.org/10.1016/j.isci.2019.10.047

proliferation, angiogenesis, and metabolism (Shen and Kaelin, 2013). Multiple lines of evidence have demonstrated that the HIF-2α subunit is the tumor promoting isoform in ccRCC (Shen and Kaelin, 2013). Because existing anti-angiogenic and mTOR-targeted therapies provide only short-term benefit, specific HIF-2 inhibitors have been developed and are in clinical trials (Chen et al., 2016; Cho et al., 2016; Wallace et al., 2016).

One puzzle in ccRCC is that neither mutations in components of PI3K/Akt/mTOR pathway nor current understanding of mTOR/HIF signaling can account for all of the elevated mTOR pathway activity found in ccRCC (Kucejova et al., 2011; Zhang et al., 2017). HIF is generally thought to inhibit mTOR by activation of regulated in development and DNA damage response 1 (REDD1) gene (Brugarolas et al., 2004). However, mTOR can evade HIF/REDD1 negative regulation in a cell line dependent manner (Kucejova et al., 2011). This suggests there must be other mechanisms of activation of mTOR in ccRCC (Elorza et al., 2012) and/or negative regulators of the pathway are suppressed. DEPTOR is found in low levels in many, but not all, cancers (Peterson et al., 2009). However, little is known about the role of DEPTOR in ccRCC. Here, we show that DEPTOR is suppressed in pVHL-inactivated ccRCC in an HIF-dependent manner. DEPTOR suppression accelerates proliferation of ccRCC cells and promotes resistance to second-generation mTOR kinase inhibitors as compensatory activation of Akt is suppressed when DEPTOR is downregulated. Our work reveals important new mechanistic insight into deregulation of mTOR in ccRCC that is mediated by HIF reprogramming of mTOR/DEPTOR signaling.

RESULTS

DEPTOR Is Suppressed in VHL-Deficient ccRCC

mTOR activity is increased in pVHL-deficient ccRCC and is a therapeutic target, but little is known about the expression of its endogenous inhibitor, DEPTOR. Microarray expression analysis using the Beroukhim renal cancer dataset (Beroukhim et al., 2009) demonstrated a significant decrease in DEPTOR mRNA in both hereditary and spontaneous VHL-deficient ccRCC tumor samples as compared with normal renal cortex (Figure 1A). Another cohort of matched ccRCC tumors and normal cortex (Gumz et al., 2007) also revealed a significant decrease in DEPTOR mRNA in 8 out of 10 samples (Figure 1B). In addition, DEPTOR mRNA and protein were strikingly suppressed in VHL-deficient ccRCC cells (786-O, RCC4) as compared with cells transfected with VHL (786-O/VHL and RCC4/VHL) as shown in Figures 1C and 1D. These results demonstrate that DEPTOR is significantly downregulated in ccRCC tumors and cell lines in a VHL-dependent manner.

DEPTOR Is Suppressed by HIFs in VHL-deficient ccRCC

Genetic alterations in PI3K/Akt/mTOR pathway components are important contributors to mTOR activation in renal cancer (Brugarolas, 2014). However, mutations in PI3K/Akt/mTOR proteins do not account for the widespread increase in mTOR pathway activity found in tumors (Zhang et al., 2017). We performed an analysis of *Deptor* genetic alterations from The Cancer Genome Atlas (TCGA) database that revealed genetic alterations in only 5 of 499 cases (1%; 4 amplifications and 1 missense mutation), which suggests that other mechanisms contribute to suppression of DEPTOR in ccRCC. Studies investigating the regulation of DEPTOR have shown it to be tightly regulated by posttranslational modification (Duan et al., 2011; Gao et al., 2011; Peterson et al., 2009; Zhao et al., 2011). Upon serum or mitogen activation, DEPTOR is rapidly phosphorylated in an mTOR-dependent manner and targeted for degradation by $SCF^{\beta TrCP}$ E3 ligase (Duan et al., 2011; Gao et al., 2011; Zhao et al., 2011). Therefore, increased mTOR activity can promote DEPTOR degradation. To test whether mTOR contributed to DEPTOR suppression, ccRCC cells were incubated with an ATP-competitive mTOR kinase inhibitor, AZD2014 (Figure 2A). As expected, AZD2014 decreased phosphorylation of mTORC1 and mTORC2 substrates, S6K1 and Akt respectively, in both VHL-deficient and VHL-competent cells. mTOR kinase ablation increased DEPTOR protein accumulation in VHL-expressing cells only (786-O/VHL and RCC4/VHL), as previously shown in other cell types that are also VHL wild type (Peterson et al., 2009), indicating that mTOR activity was not responsible for the low levels of DEPTOR observed in VHL-deficient cells (786-O and RCC4). In addition, DEPTOR is suppressed at the level of transcript (Figures 1C and S1A), and mRNA levels were not affected by AZD2014, suggesting that DEPTOR is suppressed by transcriptional or post-transcriptional mechanisms. This was supported by results showing that addition of the proteasome inhibitor, MG132, had no effect on DEPTOR protein levels in VHL-deficient 786-O cells (Figure S1B), supporting the suggestion that DEPTOR is not suppressed by posttranslational mechanisms in VHL-deficient renal cells.

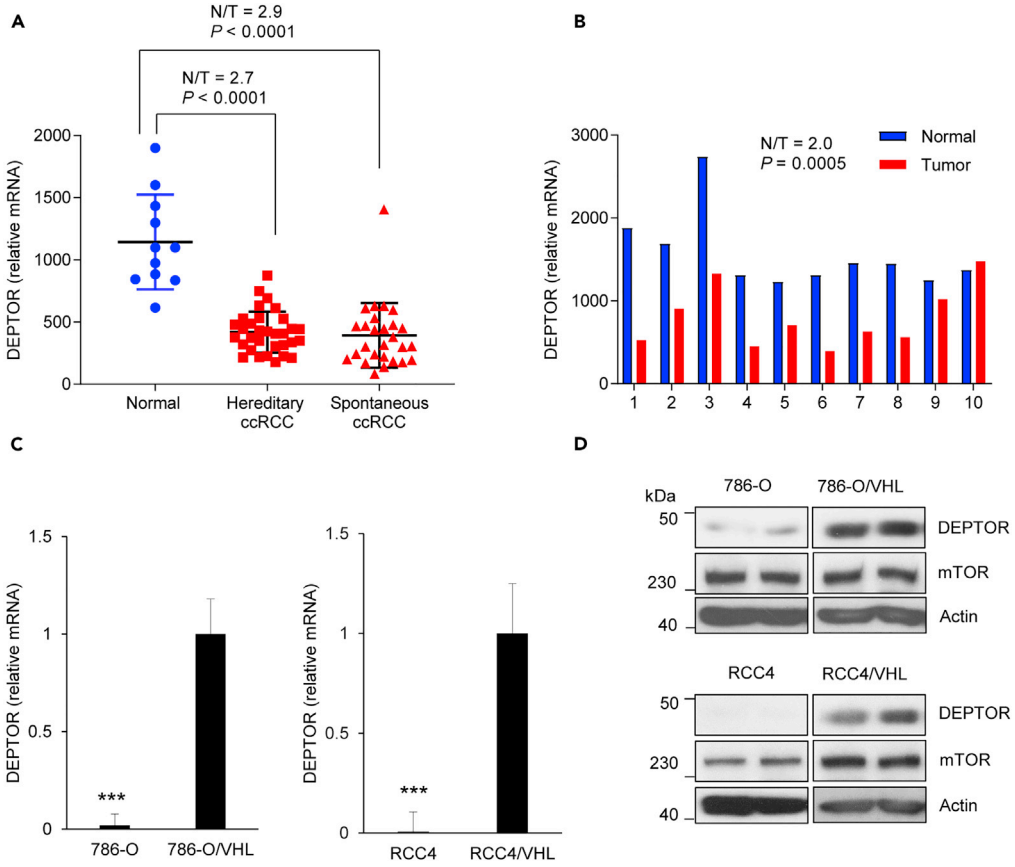

Figure 1. DEPTOR Is Downregulated in VHL-Deficient ccRCC Tumors and Cell Lines

(A) Microarray gene expression analysis of normal kidney samples (n = 11), hereditary ccRCC tumors (n = 32), and spontaneous ccRCC tumors (n = 27) extracted from dataset GSE14994 (Beroukhim et al., 2009). Statistical significance was determined by Mann-Whitney non-parametric test. N = normal; T = tumor.

(B) Microarray gene expression analysis of 10 paired ccRCC tumors and adjacent normal kidney extracted from dataset GSE6344 (Gumz et al., 2007). Statistical significance was determined by Wilcoxon matched-pairs signed rank test. N = normal; T = tumor.

(C) mRNA- from VHL-deficient ccRCC cell lines (786-O and RCC4) and cells transfected with VHL (786-O/VHL and RCC4/VHL) was analyzed for expression of DEPTOR by quantitative real-time PCR (RT-PCR) relative to GAPDH as described in Transparent Methods. Data are represented as mean ± SEM. ***p < 0.0001 by Student's two-tailed t test.

(D) Whole-cell lysates were prepared from ccRCC cell lines (786-O, 786-O/VHL, RCC4, RCC4/VHL) and were assayed by immunoblotting as described in Transparent Methods.

The data shown are representative of three independent experiments.

Loss of pVHL leads to stabilization of the transcription factors HIF-1α and HIF-2α, due to defective pVHL-mediated degradation of HIF-α subunits (Maxwell et al., 1999). Since numerous studies have identified the importance of HIF-2α in ccRCC (Shen and Kaelin, 2013), the isoform specific HIF-2 antagonist PT2385, which prevents HIF-2α from binding to ARNT/HIF-1β, was used to inhibit HIF-2 transcriptional activity (Chen et al., 2016; Wallace et al., 2016). Inhibition of HIF-2 activity by PT2385 was confirmed by measurement of HIF-2 specific target genes, vascular endothelial growth factor (VEGF), endothelin-1 (ET-1), and plasminogen activator inhibitor-1 (PAI-1), which were all significantly downregulated, demonstrating the expected effect of HIF-2 inhibition (Figure S1C). PT2385 treatment of both 786-O and RCC4 cells resulted in a marked increase in DEPTOR mRNA and protein (Figures 2B and 2C). PT2385 also inhibited HIF-2α protein accumulation, which has been noted previously (Cho et al., 2016; Wallace et al., 2016). To test whether HIF-1α was also able to inhibit DEPTOR, the effects of HIF-1α and HIF-2α ablation were investigated by siRNA-mediated knockdown (Figures 2D and 2E). Downregulation of HIFs was confirmed by RT-PCR (Figure S1D). Both HIF-1α and HIF-2α inhibition increased DEPTOR mRNA and protein, indicating that DEPTOR is suppressed by both HIFs in ccRCC (Figures 2D and 2E). To determine

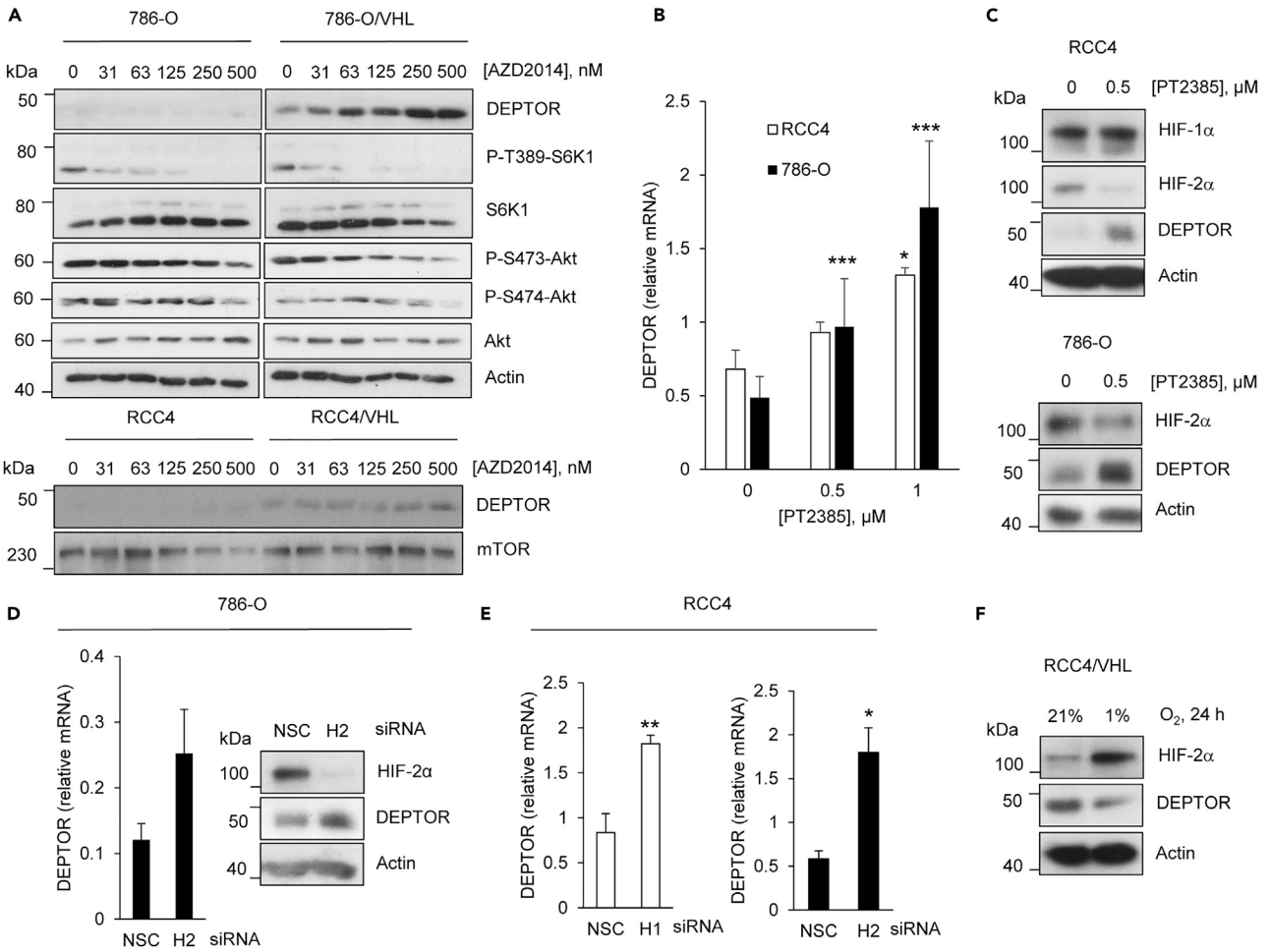

Figure 2. DEPTOR Is Suppressed by HIFs and not mTOR in VHL-Deficient ccRCC Cells

(A) VHL-deficient cells (786-O and RCC4) and VHL-expressing counterparts (786-O/VHL and RCC4/VHL) were incubated with increasing concentrations of the mTORC1/2 inhibitor, AZD2014, as indicated for 24 h. Whole-cell lysates were assessed by immunoblotting for proteins and phosphorylation states as indicated.

(B) RCC4 and 786-O cells were incubated with the HIF-2 inhibitor, PT2385, for 24 h at the concentrations indicated. mRNA expression of DEPTOR was assessed by RT-PCR relative to GAPDH. Data are represented as mean ± SEM. *$p < 0.05$; ***$p < 0.0001$ by Student's two-tailed t test.

(C) RCC4 and 786-O cells were incubated with the HIF-2 inhibitor, PT2385, for 24 h and whole-cell lysates were assessed by immunoblotting as described in Transparent Methods.

(D) 786-O cells were treated with siRNA to HIF-2α (H2) or non-silencing control (NSC) for 24 h and DEPTOR mRNA assessed by RT-PCR (graph). Data are represented as mean ± SEM. Whole-cell lysates were assessed by immunoblotting for proteins as indicated (panels).

(E) RCC4 cells were treated with siRNA to HIF-1α (H1), HIF-2α (H2), or non-silencing control (NSC) for 24 h, and DEPTOR mRNA was assessed relative to GAPDH by RT-PCR. Data are represented as mean ± SEM. *$p < 0.05$; **$p < 0.001$ by Student's two-tailed t test.

(F) RCC4/VHL cells were incubated in normoxia (21% O_2) or hypoxia (1% O_2) for 24 h and assayed by immunoblotting.

See also Figures S1 and S2.

whether DEPTOR is also suppressed by hypoxia in VHL competent cells, RCC4/VHL and 786-O/VHL cells were exposed to low oxygen tension. Hypoxia-induced DEPTOR downregulation in RCC4/VHL (Figures 2F and S2A) and 786-O/VHL cells (Figure S2B) in a time-dependant manner occurred with a concomitant stabilization of HIF-2α, indicating that DEPTOR is also repressed in cells with functional oxygen-sensing machinery. Together, these results demonstrate that DEPTOR is suppressed in an HIF-dependent manner in ccRCC.

HIF-dependent Downregulation of DEPTOR Is Mediated by BHLHe40

Previous work has demonstrated that HIFs do not function as transcriptional repressors of cognate target genes (Schödel et al., 2011) but act by induction of transcriptional intermediates (Evans et al., 2007; LaGory

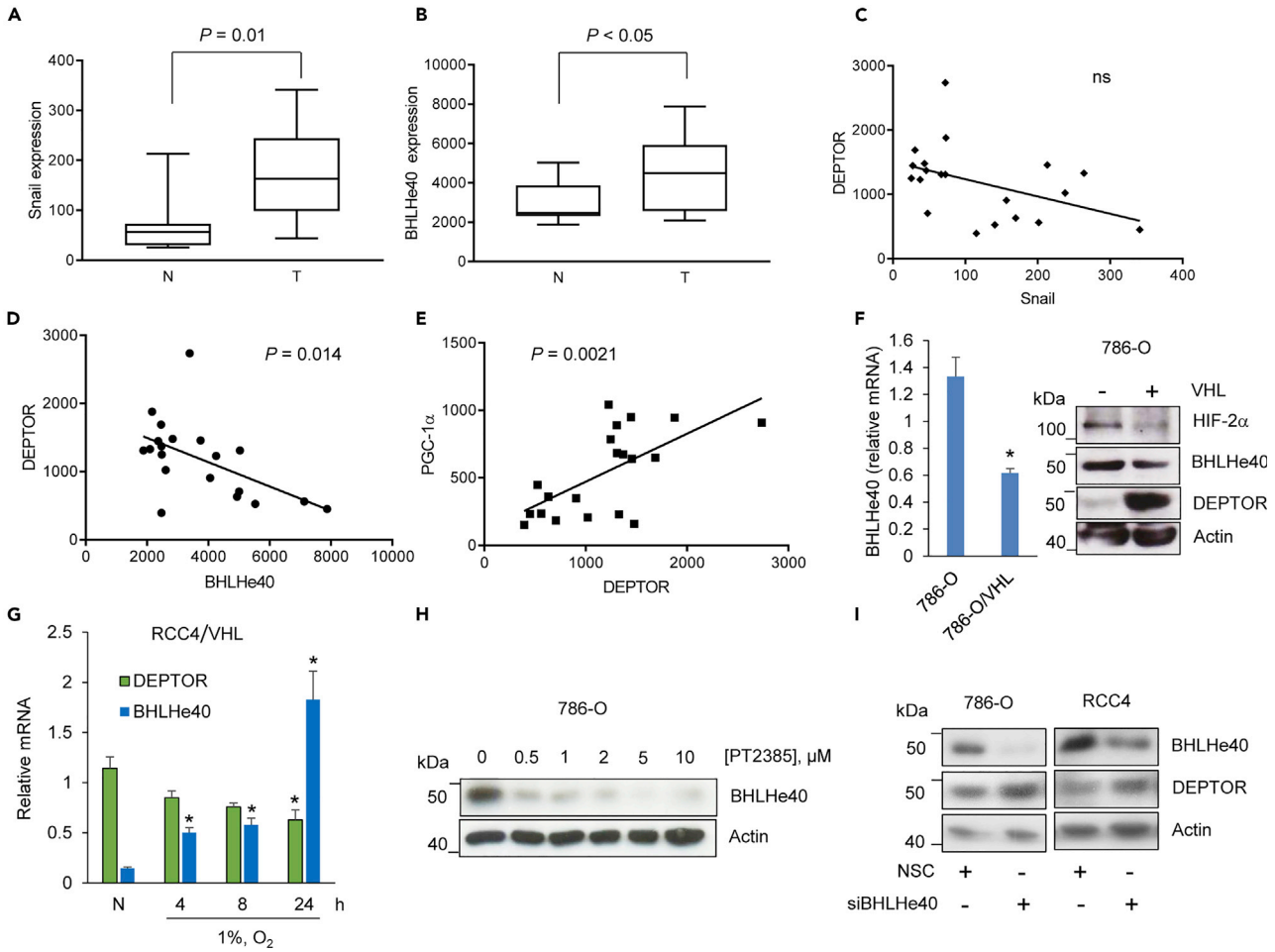

Figure 3. HIF Mediates Repression of DEPTOR by BHLHe40

(A and B) Microarray gene expression analysis of genes as indicated from matched normal kidney (N) (n = 10) and ccRCC tumors (T) (n = 10), extracted from dataset GSE6344 (Gumz et al., 2007). Statistical significance was determined by Wilcoxon matched-pairs signed rank test.

(C–E) Correlation of gene expression of genes as indicated in whole dataset of normal and ccRCC tumors (n = 20), extracted from dataset GSE6344 (Gumz et al., 2007). Statistical significance was determined by Pearson's test. NS = not significant.

(F) 786-O and 786-O/VHL cells were assessed for BHLHe40 expression. Graph. BHLHe40 mRNA levels were determined relative to GAPDH by RT-PCR. Data are represented as mean ± SEM. *p < 0.05 by Student's two-tailed t test. Panels. Immunoblotting for proteins as indicated.

(G) RCC4/VHL cells were incubated in normoxia (N, 21% O_2) for 24 h or hypoxia (1% O_2) for the times indicated, and relative mRNA levels of BHLHe40 or DEPTOR were determined relative to ribosomal L7 protein by RT-PCR. *p < 0.05 by Student's two-tailed t test.

(H) 786-O cells were incubated with increasing concentrations of PT2385 as indicated and whole-cell lysates were assessed for BHLHe40 protein by immunoblotting.

(I) Renal cells were treated with siRNA to BHLHe40 or non-silencing control (NSC) for 24 h and whole-cell lysates were assessed by immunoblotting for proteins as indicated.

See also Figure S2.

et al., 2015) or by posttranscriptional mechanisms such as induction of hypoxia-inducible microRNAs (miRNAs) (Choudhry and Mole, 2016). We investigated expression of known HIF-dependent transcriptional repressors, zinc finger protein SNAI1 (Snail) (Evans et al., 2007), and basic-helix-loop-helix family member e40 (BHLHe40) (LaGory et al., 2015). BHLHe40 is alternatively known as DEC1/Stra13/SHARP2 (Kato et al., 2014). Both Snail and BHLHe40 were upregulated in ccRCC tumors as compared with matched normal renal cortex as expected in the Gumz dataset (Gumz et al., 2007) (Figures 3A and 3B). Snail did not correlate significantly with DEPTOR expression (Figure 3C), but a significant inverse correlation of DEPTOR was found with BHLHe40 in the combined dataset of normal kidney and ccRCC tumors (n = 20) (Figure 3D). Furthermore, DEPTOR levels strongly and positively correlated with peroxisome proliferator-activated receptor-γ coactivator (PGC-1α) (Figure 3E), a gene that has previously been

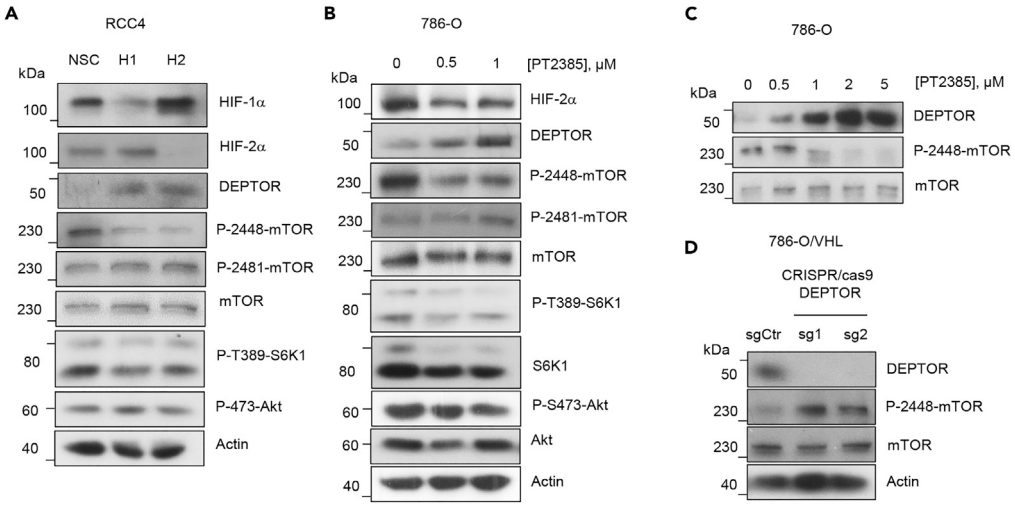

Figure 4. HIF Regulates DEPTOR and mTOR Phosphorylation at Ser2448

(A) RCC4 cells were treated with siRNA to HIF-1α (H1), HIF-2α (H2), or non-silencing control (NSC) for 24 h, and whole-cell lysates were assessed by immunoblotting for proteins and phosphorylation states as indicated.

(B and C) 786-O cells were incubated with increasing concentrations of PT2385, and whole-cell lysates were assessed by immunoblotting for proteins and phosphorylation states as indicated.

(D) Immunoblotting of CRISPR/Cas9-mediated knockout of DEPTOR in 786-O/VHL cells (sg1 and sg2) or control (sgCtr).

shown to be repressed by BHLHe40 in ccRCC (LaGory et al., 2015), suggesting a common mechanism of repression. To explore the role of BHLHe40 in DEPTOR regulation further, mRNA and protein levels were determined in renal cells. BHLHe40 was upregulated in 786-O and RCC4 cells as compared with VHL competent cells and correlated with HIF-2α as expected (Figures 3F and S2C). Re-expression of VHL resulted in diminished HIF-2α and BHLHe40 accumulation together with a concomitant increase in DEPTOR levels (Figure 3F). BHLHe40 transcript increased in a time-dependent manner in hypoxia in VHL competent cells with functional oxygen sensing machinery (Figures 3G and S2D), which corresponded with a reduction in DEPTOR (Figures 3G and S2B). We also confirmed BHLHe40 expression was dependent on HIF-2α, because it was markedly reduced by the HIF-2 inhibitor, PT2385 (Figure 3H). Finally, to confirm the role of BHLHe40 on DEPTOR suppression, VHL-deficient cells were treated with BHLHe40 siRNA. Inhibition of BHLHe40 led to increased DEPTOR accumulation in 786-O and RCC4 VHL-deficient cells (Figure 3I). Together, these results demonstrate that HIF-mediated repression of DEPTOR occurs through BHLHe40.

HIF Inhibition Increases DEPTOR Accumulation and Attenuates mTOR Phosphorylation at S2448

mTOR controls synthesis of HIF-α subunits (Toschi et al., 2008), and HIFs, in turn, have been shown to suppress mTOR activity in a negative feedback loop, likely mediated by the HIF target gene REDD1 (Brugarolas et al., 2004; Kucejova et al., 2011). However, in ccRCC, where HIFs are overexpressed, mTOR is hyperactive and has been demonstrated to evade REDD1-mediated inhibition in a cell line-dependent manner (Kucejova et al., 2011). Other mechanisms of activation of mTOR by HIFs have also been proposed in ccRCC (Elorza et al., 2012). Because DEPTOR is an endogenous mTOR inhibitor, one outcome of HIF-mediated suppression of DEPTOR in ccRCC could be increased mTOR activity. This was assessed by investigating the phosphorylation status of mTOR as well as mTORC1 and mTORC2 substrates. In line with our previous results, ablation of HIFs either by siRNAs or with PT2385 increased DEPTOR accumulation (Figures 4A–4C). The most significant change upon inhibition of HIFs was mTOR phosphorylation directly at ser2448, which was notably attenuated. By contrast, mTOR phosphorylation at ser2481 was unaffected. This suggests that HIFs can differentially affect mTOR phosphorylation status. To confirm whether DEPTOR directly prevented ser2448 mTOR phosphorylation, CRISPR/Cas 9-mediated knockout of DEPTOR was performed in VHL competent cells. Loss of DEPTOR increased ser2448 phosphorylation in VHL-expressing cells (Figure 4D). Together, these results suggest that HIFs have divergent effects on mTOR signaling and that HIF-mediated downregulation of DEPTOR in ccRCC increases mTOR phosphorylation specifically at ser2448.

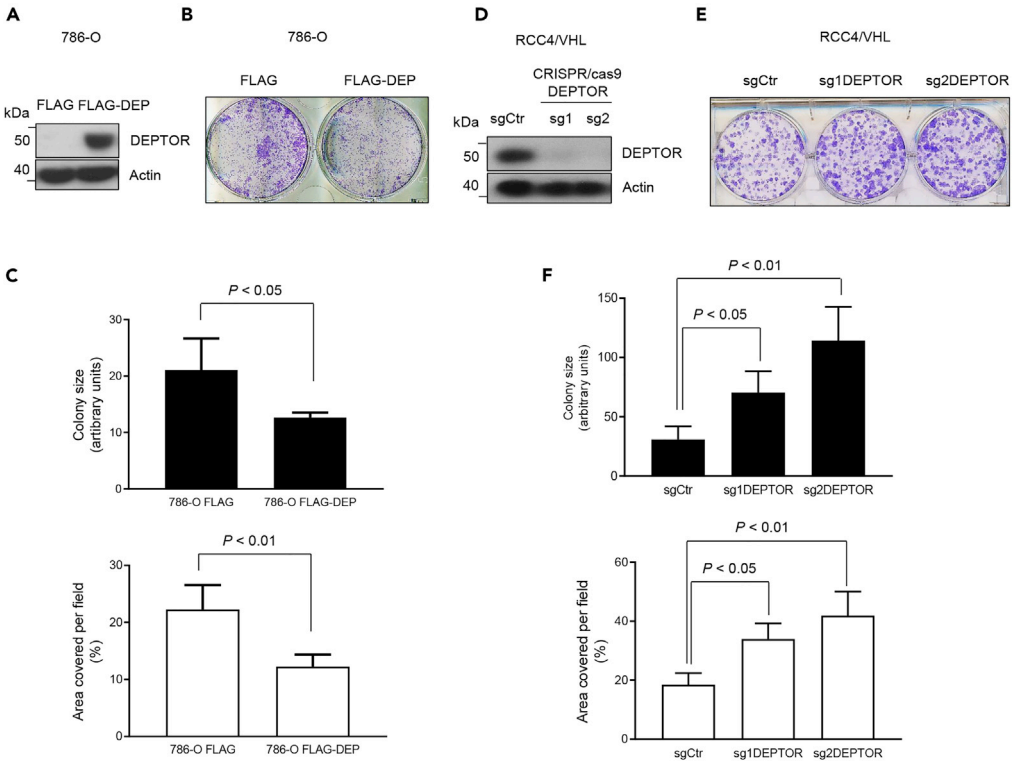

Figure 5. DEPTOR Inhibits Clonogenic Tumor Formation in ccRCC

(A) Immunoblotting of 786-O FLAG or 786-O FLAG-DEP transduced cells.

(B) Photomicrograph of clonogenic assay of 786-O FLAG or 786-O FLAG-DEP transduced cells following 10-day incubation and stained with crystal violet as described in Transparent Methods.

(C) ImageJ quantification of photomicrographs shown in B. Data are represented as Mean ± SEM of 4 quadrants. Statistical significance was determined by Student's two-tailed t test.

(D) Immunoblotting of CRISPR/Cas9 mediated knockout of DEPTOR in RCC4/VHL cells (sg1 and sg2) or control (sgCtr).

(E) Photomicrograph of clonogenic assay of RCC4/VHL cells following CRISPR/Cas9-mediated knockout of DEPTOR. Cells were stained with crystal violet following 10-day incubation.

(F) ImageJ quantification of photomicrographs shown in E. Data are represented as Mean ± SEM of four quadrants. Statistical significance was determined by Student's two-tailed t test.

Restored Expression of DEPTOR Inhibits ccRCC Tumor Colony Formation

Since DEPTOR is an mTOR inhibitor, we hypothesized that its loss in ccRCC would increase cell growth and proliferation. To test this, we restored DEPTOR expression in ccRCC cells and found that re-expression of DEPTOR inhibited ccRCC growth in a colony formation assay (Figures 5A–5C). In addition, we used CRISPR/Cas 9 gene editing to knockout DEPTOR in VHL competent cells. Consistent with an inhibitory role of DEPTOR, its loss resulted in a significant increase in size and number of tumor colonies (Figures 5D–5F).

DEPTOR Controls Feedback to IRS-2/PI3K/Akt

It is established that mTORC1 activates a negative feedback loop to inhibit upstream PI3K/Akt signaling, thereby regulating its own activity (Rozengurt et al., 2014). Previous work has demonstrated that DEPTOR is essential for coordinating the proper control of mTORC1 by dampening negative feedback to insulin receptor substrate 1 (IRS-1) (Laplante et al., 2012; Peterson et al., 2009). Specifically, the mTORC1 substrate, S6K1, phosphorylates IRS-1 at S636/639 to promote its degradation, which in turn, reduces PI3K/Akt signaling. As an mTORC1 inhibitor, DEPTOR alleviates this negative feedback loop. Therefore, when DEPTOR is manipulated in cells, its overexpression can result in increased Akt phosphorylation by dampening negative feedback. Conversely, knock down of DEPTOR reduces Akt phosphorylation as mTORC1 is active and negative feedback is predominant (Caron et al., 2018; Laplante et al., 2012; Peterson et al., 2009). These effects of DEPTOR on mTORC1 feedback seem to override its other function as an mTORC2 complex

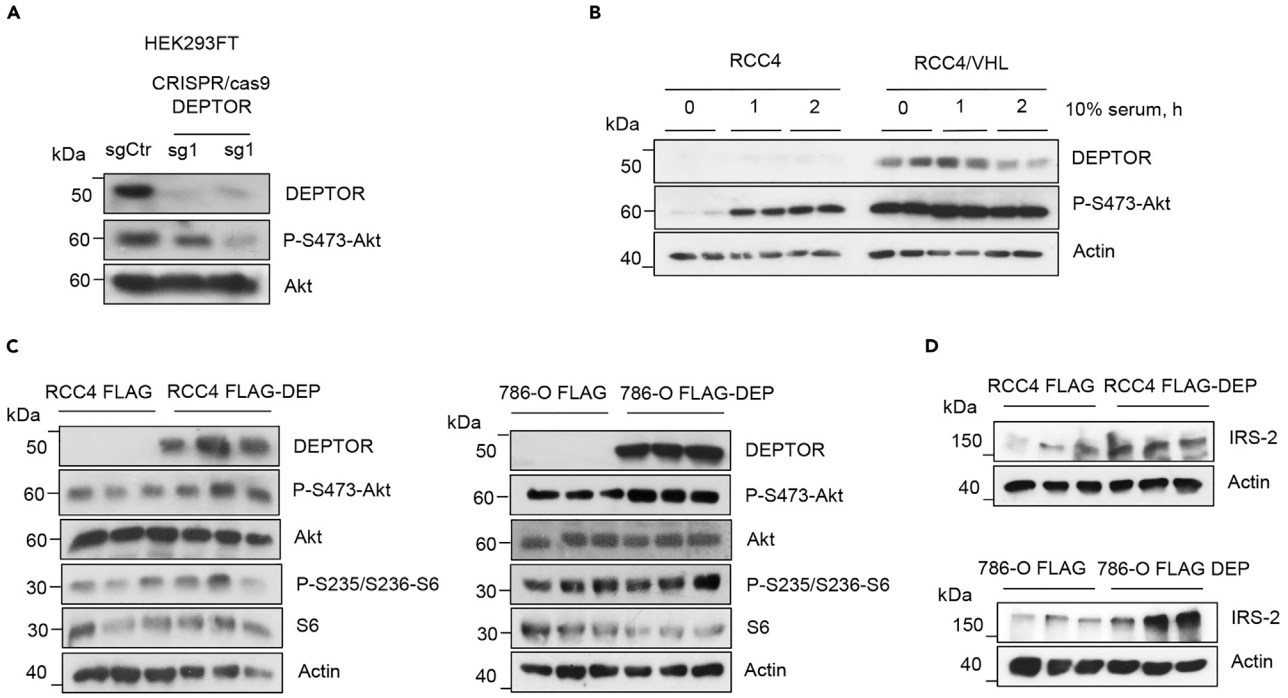

Figure 6. DEPTOR Controls Feedback to IRS-2/PI3K/Akt

(A) Immunoblotting of CRISPR/Cas9-mediated knockout of DEPTOR in HEK293FT cells (sg1 and sg2) or control (sgCtr).

(B) RCC4 and RCC4/VHL cells were serum starved for 24 h before re-addition of 10% serum for 1 or 2 h, as indicated. Whole-cell lysates were assayed by immunoblotting.

(C and D) Immunoblotting of ccRCC control cell lines (RCC4 FLAG and 786-O FLAG) or transduced with DEPTOR (RCC4 FLAG-DEP and 786-O FLAG-DEP) for proteins and phosphorylation states as indicated.

member and negative regulator (Peterson et al., 2009). We confirmed that DEPTOR affects Akt phosphorylation at S473 by generating CRISPR/Cas 9-mediated DEPTOR knockout in HEK293FT cells (Figure 6A). We then hypothesized that VHL-defective cells, with chronically suppressed DEPTOR, would have deregulated mTORC1 negative feedback signaling to PI3K/Akt. Indeed, 24 h serum deprivation led to significantly reduced Akt phosphorylation in RCC4 cells as compared with RCC4/VHL cells (Figure 6B). As expected, DEPTOR accumulates upon serum starvation in RCC4/VHL cells when HIFs are absent and is degraded upon serum stimulation. These results suggest that negative feedback by mTORC1 is amplified in VHL-deficient cells as compared with VHL competent cells because VHL-deficient cells have lost DEPTOR. We confirmed that DEPTOR was directly regulating feedback to Akt by restoring DEPTOR expression in ccRCC cells. Reintroduction of DEPTOR to RCC4 and 786-O cells increased phospho Akt without affecting other mTORC1 substrates such as phospho S6 ribosomal protein (Figure 6C). Furthermore, we show that IRS-2 levels are enhanced in DEPTOR expressing cells (Figure 6D), whereas IRS-1 levels were undetectable (data not shown), suggesting that normal feedback control to IRS-2/PI3K/Akt is deregulated in ccRCC due to depleted DEPTOR levels.

DEPTOR Loss Confers Resistance to mTOR Kinase Inhibition in ccRCC

Since DEPTOR promotes Akt activity, we predicted that mTOR kinase inhibitors that block both mTORC1 and mTORC2/Akt would be more effective in cells that express DEPTOR. Consistent with this assumption, reintroduction of DEPTOR in VHL-deficient ccRCC cells significantly enhanced the efficacy of the mTOR kinase inhibitor, AZD2014, to prevent cell proliferation (Figures 7A and 7B). By contrast, DEPTOR had no effect on rapamycin-treated cells, which predominantly inhibits mTORC1 (Figures 7C and 7D). These results demonstrate that loss of DEPTOR is a mechanism of resistance specific to mTOR kinase drugs in ccRCC.

DISCUSSION

Here, we show that DEPTOR is significantly downregulated in VHL-deficient ccRCC tumors and cell lines and that DEPTOR is transcriptionally suppressed by HIFs. Both HIF-1 and HIF-2 negatively regulate

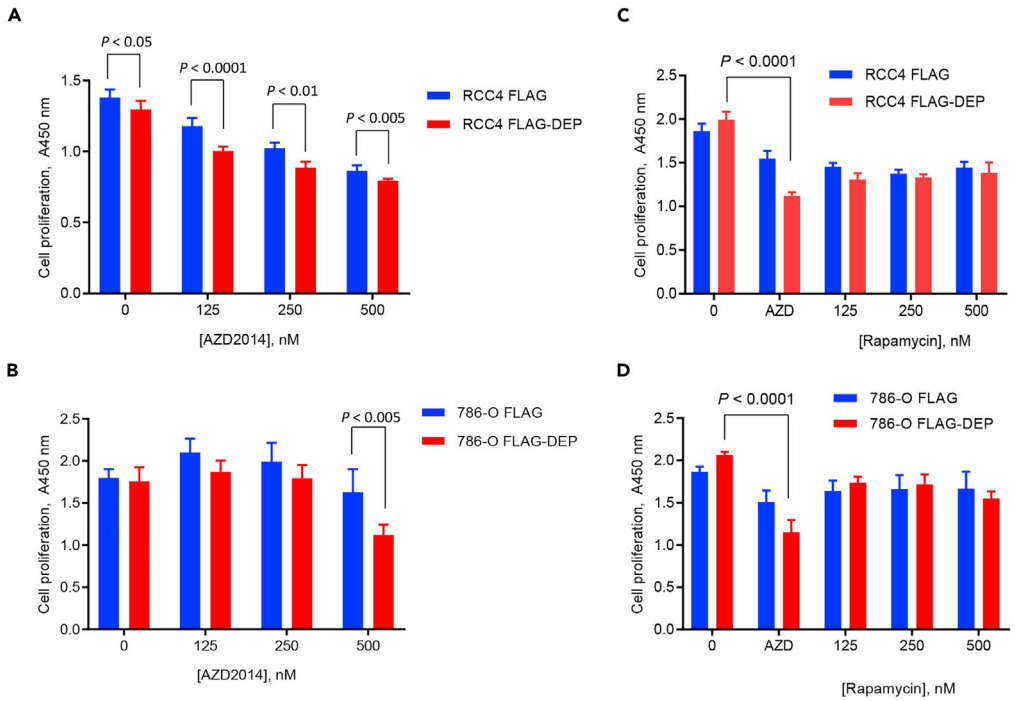

Figure 7. DEPTOR Sensitizes ccRCC Cells to mTORC1/2 Inhibition

(A and B) ccRCC control cell lines (RCC4 FLAG and 786-O FLAG) or transduced with DEPTOR (RCC4 FLAG-DEP and 786-O FLAG-DEP) were incubated with mTORC1/2 kinase inhibitor, AZD2014, at the concentrations indicated for seven days and cell proliferation determined as compared with untreated cells as described in Transparent Methods. Data are represented as mean ± SEM of six replicates. Statistical significance was determined by Student's two-tailed t test.

(C and D) Renal cells as described in (A and B) were treated with 500 nM AZD2014 (AZD) or increasing concentrations of rapamycin as indicated for seven days and cell proliferation determined as compared with untreated cells. Data are represented as mean ± SEM of six replicates. Statistical significance was determined by Student's two-tailed t test. The data shown are representative of three independent experiments.

DEPTOR, which is mediated by the HIF-target gene, BHLHe40. We further show that loss of DEPTOR leads to deregulated negative feedback to PI3K/Akt in ccRCC and resistance to second-generation mTOR kinase inhibitors that block both mTORC1 and mTORC2/Akt.

Low levels of DEPTOR have been found in a number of different tumor types (Peterson et al., 2009). However, in some cancers such as multiple myeloma, DEPTOR expression is correlated with increased tumor development, likely through enhanced PI3K/Akt (Peterson et al., 2009; Wang et al., 2012). In renal tumors, mTORC1 pathway activity is elevated in the context of HIF activation. The mechanisms of mTORC1 activation are unclear since previous work has demonstrated that HIFs negatively regulate mTOR by the HIF-target gene REDD1 (Brugarolas et al., 2004). However, in renal cancer, mTOR may evade REDD1 negative regulation and/or mTORC1 may be activated by other HIF-dependent mechanisms (Elorza et al., 2012; Kucejova et al., 2011). Our results provide evidence that mTOR activity is likely further enhanced by loss of DEPTOR in ccRCC in an HIF-dependent manner. This suggests that HIFs have multiple divergent effects on mTOR signaling pathways. We clearly show an inhibitory effect of HIFs on DEPTOR in ccRCC. This is in contrast to a previous report where hypoxia was shown to increase DEPTOR expression in HCT116 cells (Desantis et al., 2015). It is possible that the effect of HIFs on DEPTOR may be cell and context specific.

We further demonstrate that DEPTOR is repressed by the HIF-target gene, BHLHe40 (Figure 8A), which was recently shown to repress PGC-1α in ccRCC (LaGory et al., 2015). Our results are consistent with the evidence that HIFs downregulate genes indirectly and that BHLHe40 plays an important role in negative regulation of HIF target genes in ccRCC (Choudhry and Mole, 2016; LaGory et al., 2015).

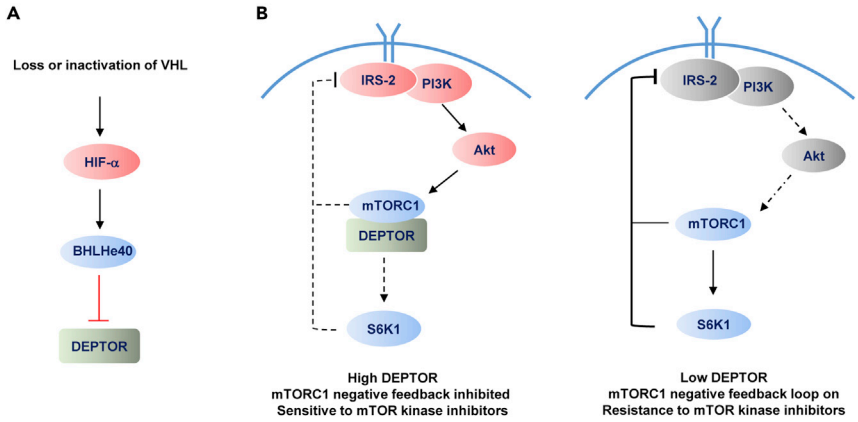

Figure 8. DEPTOR Regulates Feedback to IRS-2/PI3K/Akt in ccRCC

(A) Loss or inactivation of VHL function leads to repression of DEPTOR via HIF-mediated activation of BHLHe40.

(B) In cells with high DEPTOR levels, mTORC1 is inhibited leading to diminished negative feedback to IRS-2/PI3K. This results in enhanced Akt signaling and sensitivity to mTOR kinase inhibition. In DEPTOR-deficient cells, due to HIF-mediated repression, mTORC1 activity is enhanced leading to negative feedback to IRS-2/PI3K. This results in diminished Akt signaling and resistance to mTOR kinase inhibitors.

Through restoration and knockout experiments, we demonstrate that DEPTOR has inhibitory effects on tumor cell growth and proliferation in ccRCC in line with previous reports in other cancers (Ji et al., 2016; Li et al., 2014; Zhou et al., 2016). It is therefore possible that loss of DEPTOR contributes to ccRCC progression. In support of this notion, some activating mutations in mTOR in kidney cancer reduce binding to DEPTOR (Grabiner et al., 2014), further suggesting that DEPTOR is important in negatively regulating mTOR in ccRCC. Evidence shows that DEPTOR is critical for coordinated negative feedback signaling to IRS-1/PI3K/Akt (Laplante et al., 2012; Peterson et al., 2009). Our results are consistent with these reports, since we show that reintroduction of DEPTOR in ccRCC cells increases Akt activity and that loss of DEPTOR inhibits Akt signaling. Moreover, we show that IRS-2 levels are enhanced in DEPTOR-expressing cells, suggesting that normal feedback control to IRS-2/PI3K/Akt is deregulated in ccRCC due to depleted DEPTOR levels (Figure 8B).

Both intrinsic and acquired drug resistance are the major causes of failure of targeted therapy in cancers. In the case of allosteric mTOR inhibitors, such as derivatives of rapamycin, acquired resistance occurs from over-activation of compensatory feedback loops such as Akt when mTORC1 is inhibited (Rozengurt et al., 2014). This phenomenon led to the rationale for the design of second-generation mTOR kinase inhibitors that block both mTORC1 and mTORC2, as well as dual PI3K/mTOR inhibitors. However, in the case of ccRCC, these compounds are inferior to allosteric mTORC1 inhibitors in early clinical trials (Powles et al., 2016a, 2016b). The reasons for this are unclear. We reasoned that loss of DEPTOR would have an impact on the efficacy of mTORC1/2 inhibitors, because compensatory feedback activation of Akt is diminished in ccRCC cells. We could show that reintroduction of DEPTOR in VHL-deficient cells significantly enhanced the efficacy of AZD2014, whereas DEPTOR had no effect on the efficacy of rapamycin. Our results reveal a novel mechanism of resistance to mTORC1/2 drugs in ccRCC that is mediated by HIF-dependent rewiring of mTOR/DEPTOR networks. Importantly, these results suggest that restoration of DEPTOR may enhance the efficacy of these compounds in ccRCC.

Limitations of the Study

This study is focused on the mechanisms underlying loss of DEPTOR in well-characterized renal cancer cell lines. *In vitro* cell colony and proliferation assays point to DEPTOR deficiency having a role to play in renal cancer biology and resistance to mTOR kinase inhibitors. Data from microarray studies confirm DEPTOR is suppressed in renal cancer patients. However, further evidence would be required to confirm the role of DEPTOR in ccRCC tumor growth, mTOR dysregulation, and in response to mTOR inhibitors *in vivo* to fully clarify the role of DEPTOR in renal cancer biology.

METHODS

All methods can be found in the accompanying Transparent Methods supplemental file.

SUPPLEMENTAL INFORMATION

Supplemental Information can be found online at https://doi.org/10.1016/j.isci.2019.10.047.

ACKNOWLEDGMENTS

We thank Profs. Patrick Maxwell and William G. Kaelin, Jr. for the RCC4 and 786-O renal carcinoma cell lines respectively and Dr Christopher Carroll for critical review of the manuscript. This study was supported by the Molecular and Clinical Sciences Research Institute and the Institute of Medical and Biomedical Education, St George's, University of London. AZD2014 was obtained from Sabina Cosulich at AstraZeneca as part of an Open Innovation Project (AZ-2014-0024).

AUTHOR CONTRIBUTIONS

V.A.C. designed the experiments, performed some of the experiments, analyzed the data, and wrote the manuscript. H.D., A.P., and S.D. performed the experiments. F.M. generated plasmids and lentiviral production. J.S. performed lentiviral infections, generated cell lines, and performed cell proliferation and colony assays.

DECLARATIONS OF INTERESTS

The authors declare no competing interests.

Received: August 8, 2018
Revised: July 26, 2019
Accepted: October 23, 2019
Published: November 22, 2019

REFERENCES

Beroukhim, R., Brunet, J.P., Di Napoli, A., Mertz, K.D., Seeley, A., Pires, M.M., Linhart, D., Worrell, R.A., Moch, H., Rubin, M.A., et al. (2009). Patterns of gene expression and copy-number alterations in von-hippel lindau disease-associated and sporadic clear cell carcinoma of the kidney. Cancer Res. *69*, 4674–4681.

Brugarolas, J. (2014). Molecular genetics of clear-cell renal cell carcinoma. J. Clin.Oncol. *32*, 1968–1976.

Brugarolas, J., Lei, K., Hurley, R.L., Manning, B.D., Reiling, J.H., Hafen, E., Witters, L.A., Ellisen, L.W., and Kaelin, W.G. (2004). Regulation of mTOR function in response to hypoxia by REDD1 and the TSC1/TSC2 tumor suppressor complex. Genes Dev. *18*, 2893–2904.

Caron, A., Briscoe, D.M., Richard, D., and Laplante, M. (2018). DEPTOR at the Nexus of cancer, metabolism, and immunity. Physiol. Rev. *98*, 1765–1803.

Caron, A., Mouchiroud, M., Gautier, N., Labbé, S.M., Villot, R., Turcotte, L., Secco, B., Lamoureux, G., Shum, M., Gélinas, Y., et al. (2017). Loss of hepatic DEPTOR alters the metabolic transition to fasting. Mol. Metab. *6*, 447–458.

Chen, W., Hill, H., Christie, A., Kim, M.S., Holloman, E., Pavia-Jimenez, A., Homayoun, F., Ma, Y., Patel, N., Yell, P., et al. (2016). Targeting renal cell carcinoma with a HIF-2 antagonist. Nature *539*, 112–117.

Cho, H., Du, X., Rizzi, J.P., Liberzon, E., Chakraborty, A.A., Gao, W., Carvo, I., Signoretti, S., Bruick, R.K., Josey, J.A., et al. (2016). On-target efficacy of a HIF-2α antagonist in preclinical kidney cancer models. Nature *539*, 107–111.

Choudhry, H., and Mole, D.R. (2016). Hypoxic regulation of the noncoding genome and NEAT1. Brief Funct. Genomics *15*, 174–185.

Desantis, A., Bruno, T., Catena, V., De Nicola, F., Goeman, F., Iezzi, S., Sorino, C., Ponzoni, M., Bossi, G., Federico, V., et al. (2015). Che-1-induced inhibition of mTOR pathway enables stress-induced autophagy. EMBO J. *34*, 1214–1230.

Duan, S., Skaar, J.R., Kuchay, S., Toschi, A., Kanarek, N., Ben-Neriah, Y., and Pagano, M. (2011). mTOR generates an auto-amplification loop by triggering the βTrCP- and CK1α-dependent degradation of DEPTOR. Mol.Cell *44*, 317–324.

Elorza, A., Soro-Arnáiz, I., Meléndez-Rodríguez, F., Rodríguez-Vaello, V., Marsboom, G., de Cárcer, G., Acosta-Iborra, B., Albacete-Albacete, L., Ordóñez, A., Serrano-Oviedo, L., et al. (2012). HIF2α acts as an mTORC1 activator through the amino acid carrier SLC7A5. Mol.Cell *48*, 681–691.

Evans, A.J., Russell, R.C., Roche, O., Burry, T.N., Fish, J.E., Chow, V.W., Kim, W.Y., Saravanan, A., Maynard, M.A., Gervais, M.L., et al. (2007). VHL promotes E2 box-dependent E-cadherin transcription by HIF-mediated regulation of SIP1 and snail. Mol.Cell. Biol. *27*, 157–169.

Gao, D., Inuzuka, H., Tan, M.K., Fukushima, H., Locasale, J.W., Liu, P., Wan, L., Zhai, B., Chin, Y.R., Shaik, S., et al. (2011). mTOR drives its own activation via SCF(βTrCP)-dependent degradation of the mTOR inhibitor DEPTOR. Mol.Cell *44*, 290–303.

Grabiner, B.C., Nardi, V., Birsoy, K., Possemato, R., Shen, K., Sinha, S., Jordan, A., Beck, A.H., and Sabatini, D.M. (2014). A diverse array of cancer-associated MTOR mutations are hyperactivating and can predict rapamycin sensitivity. Cancer Discov. *4*, 554–563.

Gumz, M.L., Zou, H., Kreinest, P.A., Childs, A.C., Belmonte, L.S., LeGrand, S.N., Wu, K.J., Luxon, B.A., Sinha, M., Parker, A.S., et al. (2007). Secreted frizzled-related protein 1 loss contributes to tumor phenotype of clear cell renal cell carcinoma. Clin. Cancer Res. *13*, 4740–4749.

Ji, Y.M., Zhou, X.F., Zhang, J., Zheng, X., Li, S.B., Wei, Z.Q., Liu, T., Cheng, D.L., Liu, P., Song, K., et al. (2016). DEPTOR suppresses the progression of esophageal squamous cell carcinoma and predicts poor prognosis. Oncotarget *7*, 14188–14198.

Kato, Y., Kawamoto, T., Fujimoto, K., and Noshiro, M. (2014). DEC1/STRA13/SHARP2 and DEC2/SHARP1 coordinate physiological processes, including circadian rhythms in

response to environmental stimuli. Curr.Top Dev. Biol. *110*, 339–372.

Kucejova, B., Pena-Llopis, S., Yamasaki, T., Sivanand, S., Tran, T.A., Alexander, S., Wolff, N.C., Lotan, Y., Xie, X.J., Kabbani, W., et al. (2011). Interplay between pVHL and mTORC1 pathways in clear-cell renal cell carcinoma. Mol. Cancer Res. *9*, 1255–1265.

LaGory, E.L., Wu, C., Taniguchi, C.M., Ding, C.C., Chi, J.T., von Eyben, R., Scott, D.A., Richardson, A.D., and Giaccia, A.J. (2015). Suppression of PGC-1α is critical for reprogramming oxidative metabolism in renal cell carcinoma. Cell Rep. *12*, 116–127.

Laplante, M., Horvat, S., Festuccia, W.T., Birsoy, K., Prevorsek, Z., Efeyan, A., and Sabatini, D.M. (2012). DEPTOR cell-autonomously promotes adipogenesis, and its expression is associated with obesity. Cell Metab. *16*, 202–212.

Li, H., Sun, G.Y., Zhao, Y., Thomas, D., Greenson, J.K., Zalupski, M.M., Ben-Josef, E., and Sun, Y. (2014). DEPTOR has growth suppression activity against pancreatic cancer cells. Oncotarget *5*, 12811–12819.

Maxwell, P.H., Wiesener, M.S., Chang, G.W., Clifford, S.C., Vaux, E.C., Cockman, M.E., Wykoff, C.C., Pugh, C.W., Maher, E.R., and Ratcliffe, P.J. (1999). The tumour suppressor protein VHL targets hypoxia-inducible factors for oxygen-dependent proteolysis. Nature *399*, 271–275.

Pantuck, A.J., Seligson, D.B., Klatte, T., Yu, H., Leppert, J.T., Moore, L., O'Toole, T., Gibbons, J., Belldegrun, A.S., and Figlin, R.A. (2007). Prognostic relevance of the mTOR pathway in renal cell carcinoma: implications for molecular patient selection for targeted therapy. Cancer *109*, 2257–2267.

Peterson, T.R., Laplante, M., Thoreen, C.C., Sancak, Y., Kang, S.A., Kuehl, W.M., Gray, N.S., and Sabatini, D.M. (2009). DEPTOR is an mTOR inhibitor frequently overexpressed in multiple myeloma cells and required for their survival. Cell *137*, 873–886.

Powles, T., Lackner, M.R., Oudard, S., Escudier, B., Ralph, C., Brown, J.E., Hawkins, R.E., Castellano, D., Rini, B.I., Staehler, M.D., et al. (2016a). Randomized open-label phase II trial of apitolisib (GDC-0980), a novel inhibitor of the PI3K/mammalian target of rapamycin pathway, versus everolimus in patients with metastatic renal cell carcinoma. J. Clin.Oncol. *34*, 1660–1668.

Powles, T., Wheater, M., Din, O., Geldart, T., Boleti, E., Stockdale, A., Sundar, S., Robinson, A., Ahmed, I., Wimalasingham, A., et al. (2016b). A randomised phase 2 study of AZD2014 versus everolimus in patients with VEGF-refractory metastatic clear cell renal cancer. Eur. Urol. *69*, 450–456.

Rozengurt, E., Soares, H.P., and Sinnet-Smith, J. (2014). Suppression of feedback loops mediated by PI3K/mTOR induces multiple overactivation of compensatory pathways: an unintended consequence leading to drug resistance. Mol. Cancer Ther. *13*, 2477–2488.

Saxton, R.A., and Sabatini, D.M. (2017). mTOR signaling in growth, metabolism, and disease. Cell *169*, 361–371.

Schödel, J., Oikonomopoulos, S., Ragoussis, J., Pugh, C.W., Ratcliffe, P.J., and Mole, D.R. (2011). High-resolution genome-wide mapping of HIF-binding sites by ChIP-seq. Blood *117*, e207–e217.

Shen, C., and Kaelin, W.G., Jr. (2013). The VHL/HIF axis in clear cell renal carcinoma. Semin. Cancer Biol. *23*, 18–25.

Toschi, A., Lee, E., Gadir, N., Ohh, M., and Foster, D.A. (2008). Differential dependence of hypoxia-inducible factors 1 alpha and 2 alpha on mTORC1 and mTORC2. J. Biol. Chem. *283*, 34495–34499.

Wallace, E.M., Rizzi, J.P., Han, G., Wehn, P.M., Cao, Z., Du, X., Cheng, T., Czerwinski, R.M., Dixon, D.D., Goggin, B.S., et al. (2016). A small-molecule antagonist of HIF2α is efficacious in preclinical models of renal cell carcinoma. Cancer Res. *76*, 5491–5500.

Wang, Z., Zhong, J., Inuzuka, H., Gao, D., Shaik, S., Sarkar, F.H., and Wei, W. (2012). An evolving role for DEPTOR in tumor development and progression. Neoplasia *14*, 368–375.

Zhang, Y., Kwok-Shing Ng, P., Kucherlapati, M., Chen, F., Liu, Y., Tsang, Y.H., de Velasco, G., Jeong, K.J., Akbani, R., and Hadjipanayis, A. (2017). A pan-cancer proteogenomic Atlas of PI3K/AKT/mTOR pathway alterations. Cancer Cell *31*, 820–832.e3.

Zhao, Y., Xiong, X., and Sun, Y. (2011). DEPTOR, an mTOR inhibitor, is a physiological substrate of SCF(βTrCP) E3 ubiquitin ligase and regulates survival and autophagy. Mol.Cell *44*, 304–316.

Zhou, X., Guo, J., Ji, Y., Pan, G., Liu, T., Zhu, H., and Zhao, J. (2016). Reciprocal negative regulation between EGFR and DEPTOR plays an important role in the progression of lung adenocarcinoma. Mol. Cancer Res. *14*, 448–457.

ISCI, Volume *21*

Supplemental Information

HIF-mediated Suppression of DEPTOR Confers Resistance to mTOR Kinase Inhibition in Renal Cancer

Hong Doan, Alexander Parsons, Shruthi Devkumar, Jogitha Selvarajah, Francesc Miralles, and Veronica A. Carroll

Supplemental Figures

Figure S1

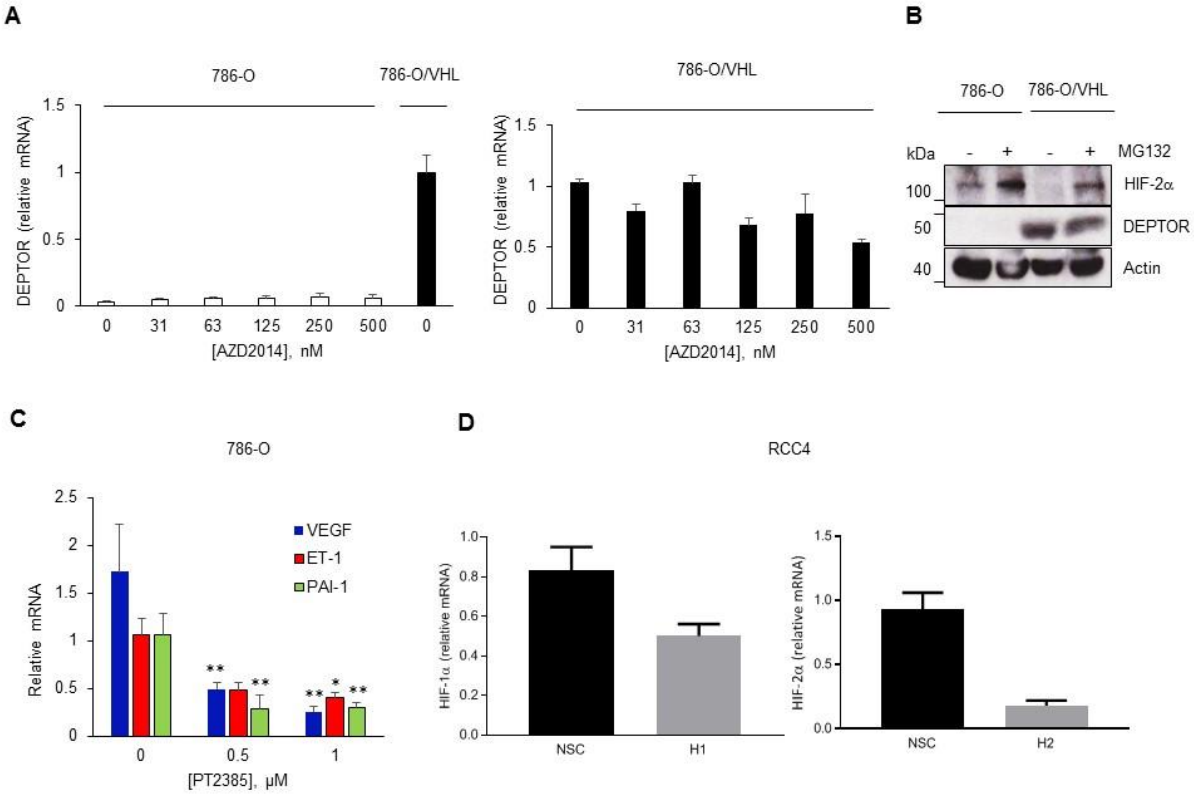

Figure S1. DEPTOR is regulated at the level of transcript in VHL-deficient cells.

Related to Figure 2.

(A) 786-O and 786-O/VHL cells were incubated with AZD2014 for 24 h and DEPTOR mRNA was assessed by RT-PCR relative to GAPDH.

(B) 786-O and 786-O/VHL cells were incubated with 10 μM MG132 for 3 h and whole-cell lysates assessed by immunoblotting.

(C) 786-O cells were treated with the HIF-2 inhibitor, PT2385, for 24 h at the concentrations indicated. mRNA expression of HIF target genes was assessed by RT-PCR relative to GAPDH.

(D) RCC4 cells were treated with siRNA to HIF-1α (H1), HIF-2α (H2) or non-silencing control (NSC) for 24 h and mRNA expression was assessed by RT-PCR relative to GAPDH.

Data are represented as mean ± SEM. *$p < 0.05$; **$p < 0.001$ by Student's two-tailed t test.

Figure S2

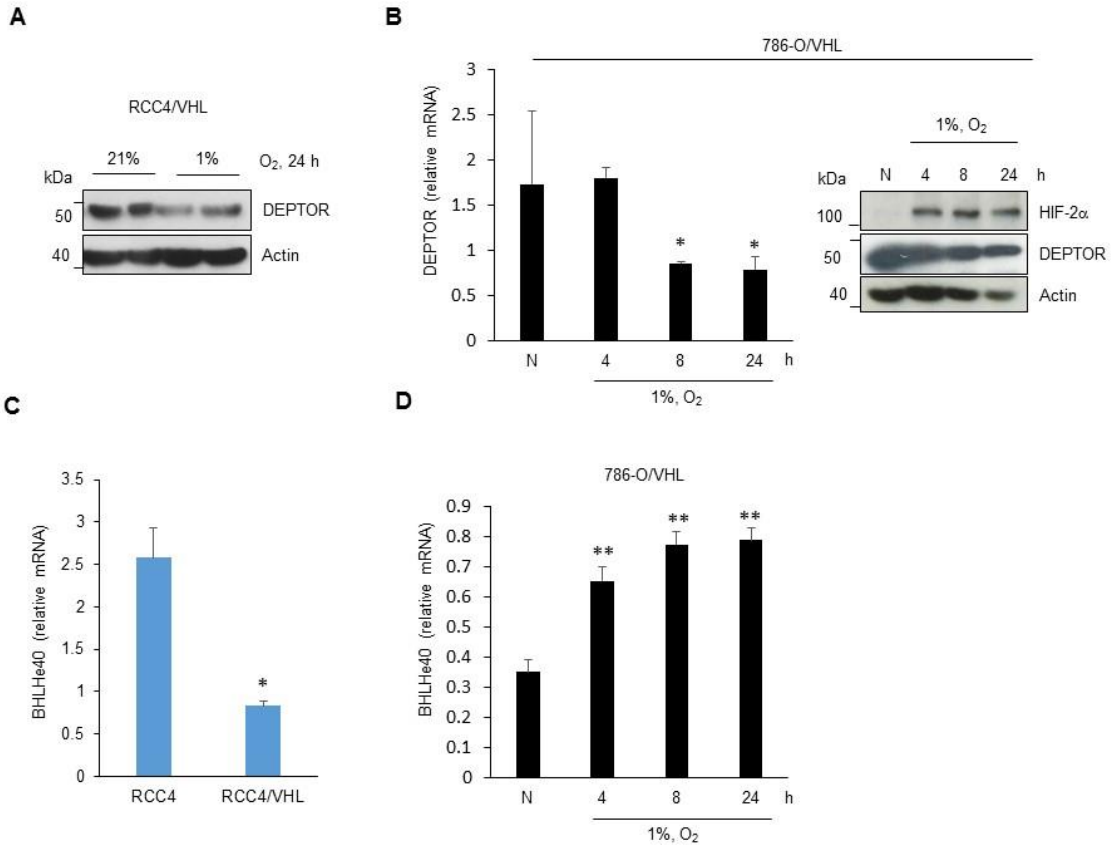

Figure S2. Downregulation of DEPTOR by hypoxia. Related to Figures 2 and 3.

(A) RCC4/VHL cells were incubated in normoxia, (21% O_2) or hypoxia (1% O_2) for 24 h. Whole-cell lysates were assessed by immunoblotting.

(B) 786-O/VHL cells were incubated in normoxia, N (21% O_2) for 24 h, or hypoxia (1% O_2) for the times indicated. Graph. DEPTOR mRNA levels were determined by RT-PCR relative to ribosomal L7 protein. Panels. Whole-cell lysates were assessed by immunoblotting.

(C) RCC4 and RCC4/VHL cells were assessed for expression of BHLHe40 mRNA by RT-PCR relative to GAPDH.

(D) 786-O/VHL cells were incubated in normoxia, N (21% O_2) or hypoxia (1% O_2) for the times indicated. BHLHe40 mRNA levels were determined relative to ribosomal L7 protein by RT-PCR.

Data are represented as mean ± SEM. *$p < 0.05$; **$p < 0.001$ by Student's two-tailed t test.

Transparent methods

Reagents

The mTOR kinase inhibitor, AZD2014 was kindly provided by Sabina Cosulich AstraZeneca. The HIF-2 inhibitor, PT2385 was purchased from Insight Biotechnology, Wembley, UK. Rapamycin was purchased from Cambridge Bioscience, Cambridge, UK. MG132 was purchased from Sigma-Aldrich, Gillingham, UK.

Cell Culture

Cell lines were maintained in Dulbecco's modified Eagle medium (Hyclone, GE Healthcare, UK) supplemented with 10% fetal bovine serum (Sigma-Aldrich, Gillingham, UK), 100 IU/mL penicillin, 100 µg/mL streptomycin, 2 mM glutamine (all purchased from Life Technologies, Paisley, UK) and amphotericin B (Sigma-Aldrich, Gillingham, UK). Matched RCC4 renal cell carcinoma cells (RCC4 and RCC4/VHL) were gifts from Professor Patrick Maxwell (Cambridge University, UK). The 786-O renal cell carcinoma cells (786-O and 786-O/VHL) were gifts from Professor William G. Kaelin Jr (Dana-Farber Cancer Institute, Harvard Medical School, Boston, MA, USA).

Plasmid generation and lentiviral production

DEPTOR overexpression and knockout cell lines were generated by lentiviral transduction. Plasmid pLJM60 was a gift from David Sabatini (Addgene #34610) and used to overexpress epitope-tagged FLAG-DEPTOR (FLAG-DEP). A negative control

plasmid expressing the FLAG-epitope only (FLAG) was generated by excising the DEPTOR cDNA with SalI and NotI enzymes, filling in the ends and recircularising the vector backbone. For the generation of human DEPTOR knockouts, two independent sgRNAs (5'GCAGCACCAGCGGGAGTGGC3' and 5'GCAAAGGGAGCTGGAGCGCA3') (sg1DEPTOR and sg2DEPTOR) were designed using the E-crisp sgRNA-designer tool (Heigwer et al., 2014) and cloned into lenti-CRISPR-v2 plasmid (Addgene #52961) (Sanjana et al., 2014). A non-targeting sgRNA was used as a negative control (sgCtr). Lentiviral particles were generated as previously described (Shi et al., 2016). Two days after viral transduction, infected cells were selected with 2 µg/mL puromycin (Sigma-Aldrich) and expanded.

siRNA duplexes and transient transfections

Cells were transfected with siRNA duplexes using HiPerfect (QIAGEN, Crawley, UK) transfection reagent according to manufacturer's instructions. siRNA duplexes to DEPTOR (sc-77660), HIF-1α (sc-35561), HIF-2α (sc-35316) and BHLHe40/DEC1/Stra13 (sc-106769) were obtained from Santa Cruz (Insight Biotechnology, UK). AllStars negative control siRNA duplex was used as a non-silencing control (NSC) and obtained from QIAGEN. Cells were seeded onto six-well culture dishes at a confluence of 50%. Before transfection, cells were washed twice with PBS, and duplexes were added to wells at 10 nM in DMEM supplemented with 10% fetal bovine serum for 24 hours at 37°C and 5% CO_2.

Hypoxic Induction

Cells were exposed to hypoxia (1% O_2, 5% CO_2, and 94% N_2) for the times indicated in figure legends in a Galaxy48R New Brunswick incubator (Eppendorf, Stevenage,

UK) at 37°C.

Immunoblotting

Following cell treatments as describe in figure legends, cells were placed on ice, washed twice with ice-cold PBS and whole-cell lysates were prepared by cell lysis in 2x Laemmli buffer (4% w/v SDS, 20% v/v glycerol, 120 mM tris pH 6.8) as previously described (Valentine et al., 2011). To determine protein concentration, 5 µL of each sample was diluted in 95 µL dH_20, and added to 1 mL Lowry solution (50 parts 2% w/v sodium carbonate, 0.1 M sodium hydroxide solution, to 1 part 0.5% w/v copper(II)sulphate, 1% w/v sodium citrate solution) and incubated at room temperature for 10 mins. 100 µL of 1 M Folin-Ciocalteau solution was added, and further incubated for 30 mins at room temperature. Protein concentration was determined using a CamSpec-M330 spectrometer. Samples of equal protein concentration were loaded onto 10% polyacrylamide gels and underwent electrophoresis, followed by transfer onto polyvinylidene difluoride (PVDF) membrane (GE Healthcare) by semi-dry electroblotting using BioRad Trans-Blot® SD Semi-Dry Transfer Cell. Membranes were blocked with 5% milk/TBS-T solution (5%w/v Marvel milk powder in 1X TBS-T solution comprising 50 mM Tris, 150 mM sodium chloride, 0.364% v/v hydrochloric acid, 0.5% v/v Tween-20) and probed overnight at 4°C for specific proteins of interest as described below. Standard primary antibody dilutions were performed in 5% milk/TBS-T solution. Secondary antibody dilutions were prepared in 5% milk/TBS-T solution. Chemiluminescence was detected using LumiGLO® chemiluminescent regent (Cell Signaling Technology, USA) according to manufacturer's instructions, exposed to hyperfilm (GE Healthcare, Buckinghamshire, UK) and were developed using an Amersham SRX100A Hyperprocessor.

HIF-1α antibody was purchased from BD Biosciences (Oxford, UK). HIF-2α antibody (NB100-122) and BHLHe40/DEC1 antibody (NB100-1800SS) were purchased from Novus Biologicals (Cambridge, UK). Actin antibody (AC-15), IRS-1 (H-7) and IRS-2 (B-5) were purchased from Santa Cruz. Antibodies recognizing DEPTOR (D9F5), mTOR (7C10), S6K1 (p70S6K)(49D7), Akt (9272), S6 (5G10) and anti-phospho-antibodies S-2448-mTOR (2971), S2481-mTOR (2974), T-389-S6K1 (49D7), S-473-Akt (D9E), S-474-Akt2 (D3H2) and S-235/236-S6 (2211) were all obtained from Cell Signaling, New England Biolabs, Hitchin, UK.

Quantitative real-time PCR assays

Total RNA was extracted from cells using RNeasy Mini Kit (QIAGEN) and 50 ng total RNA was used for first-strand cDNA synthesis using the Sensiscript™ reverse transcriptase kit (QIAGEN) according to manufacturer's instructions. Real-time PCR was performed with GoTaq™ qPCR master mix (Promega, Southampton, UK) in a Biorad CFX connect real time cycler. All primers were purchased from Sigma-Aldrich as described below. Expression level of each gene was normalized to GAPDH or ribosomal L7 protein as described in the figure legends.

DEPTOR (forward 5'-TTTGTGGTGCGAGGAAGTAA; reverse 5'-CATTGCTTTGTGTCATTCTGG)

HIF-1α (forward 5′-GCAAGCCCTGAAAGCG; reverse 5′-GGCTGTCCGACTTTGA

HIF-2α (forward 5′-GTCTCTCCACCCCATGTCTC; reverse 5′-GGTTCTTCATCCGTTTCCAC)

VEGF (forward 5′-TACCTCCACCATGCCAAGTG; reverse 5′-ATGATTCTGCCCTCCTCCTTC)

PAI-1 (forward 5′-TCTTTGGTGAAGGGTCTGCT; reverse 5′-CTGGGTTTCTCCTCCTGTTG)
Endothelin-1 (forward 5′-TGGACATCATTTGGGTCAACA; reverse 5′-TCTCTTGGACCTAGGGCTTCC)
GAPDH (forward 5′-ATGGGGAAGGTGAAGGTCG; reverse 5′-TAAAAGCAGCCCTGGTGACC)
Ribosomal L7 protein (forward 5'-AAGATCAAGCGCCTGAGAAAG; reverse 5'-TGCAGGTACATAGAAGTTGCCA)

Colony Assays

50 cells per well were seeded in 6 well plates in DMEM and 10% FBS and incubated for 10 days. Medium was removed and cells were fixed and stained with 0.01% crystal violet (Sigma-Aldrich), 1% formaldehyde, 1% methanol in PBS for 20 mins at room temperature. Staining solution was removed and plates were washed in distilled water and air-dried. Colonies were quantified using Image J software (National Institutes of Health, Bethesda, Maryland, USA).

Cell proliferation assays

Cells were seeded at $3x10^3$ cells per well in 96 well plates overnight in DMEM and 10% FBS. Medium was replaced and cells were incubated with test reagents as indicated in the figure legends for 7 days before addition of CellTiter 96 Aqueous One Solution Cell Proliferation Assay (Promega, Hampshire, UK) according to manufacturer's instructions.

Statistical analysis

Statistical analysis was performed using GraphPad Prism™. P values of <0.05 were considered statistically significant.

Supplemental References

Heigwer, F., Kerr, G., and Boutros, M. (2014). E-CRISP: fast CRISPR target site identification. Nat Methods *11*, 122-123.

Peterson, T.R., Laplante, M., Thoreen, C.C., Sancak, Y., Kang, S.A., Kuehl, W.M., Gray, N.S., and Sabatini, D.M. (2009). DEPTOR is an mTOR inhibitor frequently overexpressed in multiple myeloma cells and required for their survival. Cell *137*, 873-886.

Sanjana, N.E., Shalem, O., and Zhang, F. (2014). Improved vectors and genome-wide libraries for CRISPR screening. Nat Methods *11*, 783-784.

Selvarajah, J., Nathawat, K., Moumen, A., Ashcroft, M., and Carroll, V.A. (2013). Chemotherapy-mediated p53-dependent DNA damage response in clear cell renal cell carcinoma: role of the mTORC1/2 and hypoxia-inducible factor pathways. Cell Death Dis *4*, e865.

Shi, J., Miralles, F., Birnbaumer, L., Large, W.A., and Albert, A.P. (2016). Store depletion induces Gαq-mediated PLCβ1 activity to stimulate TRPC1 channels in vascular smooth muscle cells. FASEB J *30*, 702-715.

Valentine, J.M., Kumar, S., and Moumen, A. (2011). A p53-independent role for the MDM2 antagonist Nutlin-3 in DNA damage response initiation. BMC Cancer *11*, 79.